Highly sensitive photoassociation spectroscopy of ultracold $^{23}Na^{133}Cs$ molecular long-range states below the $3S_{1/2}+6P_{3/2}$ limit*

Yanyan Liu(刘艳艳)[1,2], Jizhou Wu(武寄洲)[1,2,†], Wenliang Liu(刘文良)[1,2], Xiaofeng Wang(王晓锋)[1,2], Wenhao Wang(王文浩)[1,2], Jie Ma(马杰)[1,2], Liantuan Xiao(肖连团)[1,2], and Suotang Jia(贾锁堂)[1,2]

[1] *State Key Laboratory of Quantum Optics and Quantum Optics Devices, Institute of Laser Spectroscopy, Shanxi University, Taiyuan* 030006, *China*
[2] *Collaborative Innovation Center of Extreme Optics, Shanxi University, Taiyuan* 030006, *China*

(Received 27 September 2017; revised manuscript received 23 October 2017; published online 20 November 2017)

We present high resolution photoassociation spectroscopy of ultracold $^{23}Na^{133}Cs$ molecules in a long-range $c^3\Sigma^+$ state below the $(3S_{1/2}+6P_{3/2})$ asymptote. We perform photoassociation spectroscopy in a dual-species magneto-optical trap (MOT) and detect the photoassociation resonances using trap-loss spectroscopy. By fitting the experimental data with the semi-classical LeRoy–Bernstein formula, we deduce the long-range molecular coefficient C_6 and derive the empirical potential energy curve in the long-range region.

Keywords: ultracold molecule, photoassociation, high-resolution spectroscopy, C_6 coefficient

PACS: 37.10.Pq, 33.15.Mt, 33.80.Wz **DOI:** 10.1088/1674-1056/26/12/123702

1. Introduction

Ultracold polar molecules have received considerable attention due to their versatile applications in controlled ultracold chemistry,[1] quantum simulations,[2] precision measurements,[3] and quantum information.[4] However, it is only recently that a few of these molecules (KRb, RbCs, NaK, NaRb) were successfully prepared in their rovibrational ground states. In the experiments to produce ultracold polar molecules, the ultracold atoms were first associated to form weakly bound molecules by tuning a magnetic Feshbach resonance, and then the molecules were optically transferred to the ground state in virtue of an optimized excited state. For a few molecular species, the Feshbach resonances are absent or hard to access experimentally. Thus, it is more convenient to produce molecules in the electronic ground state by using light-assisted processes, which involve coupling the atomic ground state to the excited molecular state, such as KRb,[5] LiCs,[6] and RbCs.[7] Whenever light is used to prepare ultracold polar molecules in a controlled way or to manipulate their internal state, precise knowledge of their molecular level structures is required, not only the electronic ground state, but also the excited state. One of the methods for obtaining this information is photoassociation (PA) spectroscopy, where ultracold atoms are coupled to the excited molecular states using a resonant laser. The PA spectroscopy offers a unique chance to probe the molecular long-range states and determine the molecular coefficients[8,9] and the potential energy curve.[10,11]

Our choice of polar molecule, $^{23}Na^{133}Cs$, has a relatively large electric dipole moment of ~ 4.6 Debye (which is only exceeded by the value of LiCs among all bi-alkali molecules), and is collisionally chemical stable,[12] which makes it a promising candidate for the various applications mentioned above. Nevertheless, NaCs is still one of the least experimentally explored bi-alkali molecules, and no ultracold NaCs molecules were previously prepared in their rovibrational ground state. Thus, accurate spectroscopic information is required for the production of such molecules. Bigelow and co-workers reported, for the first time, the observation of ultracold NaCs using spectroscopy via a PA experiment.[13] The PA spectroscopy of the partially excited electronic states of NaCs molecules was obtained using ionization detection.[14–16] However, the photoionization spectroscopy does not provide information about the PA transition intensities due to the intervention of the extra ionization laser,[17] and it can only obtain partial molecular states.[18] A feasible technique is the trap-loss detection, which is achieved by directly monitoring the fluorescence from the trapped atoms. In our effort to create ultracold ensembles of NaCs molecules, we have previously performed PA on ultracold Na and Cs atoms in a dual-species magneto-optical trap (MOT), where we obtained the energy positions of the weakly bound levels in the excited $c^3\Sigma^+$ state of NaCs molecules using trap-loss spectroscopy.[19] In addition, we have reported the experimental observation of the laser-induced frequency shift of NaCs molecules by collection of trap-loss spectra.[20] It should

*Project supported by the National Key Research and Development Program of China (Grant No. 2017YFA0304203), the ChangJiang Scholars and Innovative Research Team in the University of the Ministry of Education of China (Grant No. IRT13076), the National Natural Science Foundation of China (Grant Nos. 91436108, 61378014, 61675121, 61705123, and 11434007), the Fund for Shanxi "1331 Project" Key Subjects Construction, China, and the Foundation for Outstanding Young Scholars of Shanxi Province, China (Grant No. 201601D021001).

†Corresponding author. E-mail: wujz@sxu.edu.cn

© 2017 Chinese Physical Society and IOP Publishing Ltd

be noted that, although the information of NaCs's molecular hyperfine structure in the ionization/trap-loss spectrum has been previously obtained, no detailed study on the long-range molecular coefficients and the potential energy curve of the ^{23}Na^{133}Cs molecules has been reported.

In this paper, we perform PA spectroscopy in a dual-species ^{23}Na–^{133}Cs MOT and detect the PA resonances of ^{23}Na^{133}Cs's molecular $c^3\Sigma^+$ long-range state below the $(3S_{1/2}+6P_{3/2})$ limit using the trap-loss spectroscopy. By observing and analyzing the molecular hyperfine structure from the trap-loss spectrum, we extract information about the energetic position of the molecular rovibrational levels. By using the semi-classical LeRoy–Bernstein (LRB) formula,[21] we obtain the accurate long-range molecular coefficient C_6, and deduce the long-range parts of the potential energy curves. We also make a comparison of our results with other experimental and theoretical values. This work provides accurate spectroscopic information, and it is the first important step towards creating ultracold ground-state ^{23}Na^{133}Cs molecules.

2. Experimental setup

Our experiments were performed in a dual-species ^{23}Na–^{133}Cs MOT with a background pressure of about 6×10^{-7} Pa, which allowed us to obtain a large number of ultracold atoms with minimal losses from light-assisted interspecies collisions.[22] The details of the apparatus are shown schematically in Fig. 1. The magnetic field for the MOT was generated by a pair of anti-Helmholtz coils with a typical gradient of 15 Gs/cm (1 Gs $=10^{-4}$ T) along the axis of the coils. The Cs trapping and repumping beams were provided by two Littrow external-cavity diode lasers (DL100 pro, Toptica; Laser diode, Eagleyard), and the Na trapping and repumping beams were provided by a high-power, tunable, frequency-doubled diode laser (TA-SHG pro, Toptica). They were all locked using the saturation-absorption spectroscopy technique. By adjusting the acousto-optic modulators (AOMs), the frequencies of the Na and Cs trapping beams were tuned to 15 MHz and 10 MHz below the atomic hyperfine resonance transitions $3S_{1/2}(F=2)\rightarrow3P_{3/2}(F'=3)$ (~16973.343 cm^{-1}) and $6S_{1/2}(F=4)\rightarrow6P_{3/2}(F'=5)$ (~11732.176 cm^{-1}), respectively. The Na and Cs repumping beams were resonant against the $3S_{1/2}(F=1)\rightarrow3P_{3/2}(F'=2)$ (~16973.402 cm^{-1}) and $6S_{1/2}(F=3)\rightarrow6P_{3/2}(F'=4)$ (~11732.478 cm^{-1}) transitions, respectively. The diameter of the mixed atomic cloud load was approximately 1.2 mm. As a result, the ^{23}Na–^{133}Cs MOT typically had $N_{\rm Na}\approx9\times10^6$ ($N_{\rm Cs}\approx6\times10^7$) with a density of 2.0×10^9 cm^{-3} (1.5×10^9 cm^{-3}), where the majority of the Na (Cs) atoms were at the lower $F=1$ ($F=3$) hyperfine levels of the $3s^2S_{1/2}$ state ($6s^2S_{1/2}$ state). The temperature of the ultracold Na (Cs) atomic sample was measured to be about 150 μK (120 μK) by using the time-of-flight method. The overlap of the dual-species MOT was verified using the two charge-coupled device (CCD) cameras that were placed along the horizontal and vertical directions.

The PA laser was provided by a widely tunable continuous-wave Ti:sapphire laser system (MBR 110, Coherent) with a typical linewidth of ~100 kHz and an output power up to ~3.5 W. The long time frequency drift of the laser was suppressed to within 500 kHz by locking to its self-reference cavity. The absolute frequency of the PA laser was measured with a wavelength meter (High Finesse-Angstrom WS/U) that had an accuracy of 30 MHz. The PA laser beam was collimated to a $1/e^2$ diameter of 0.78 mm and had a maximum available average intensity of ~750 W/cm^2.

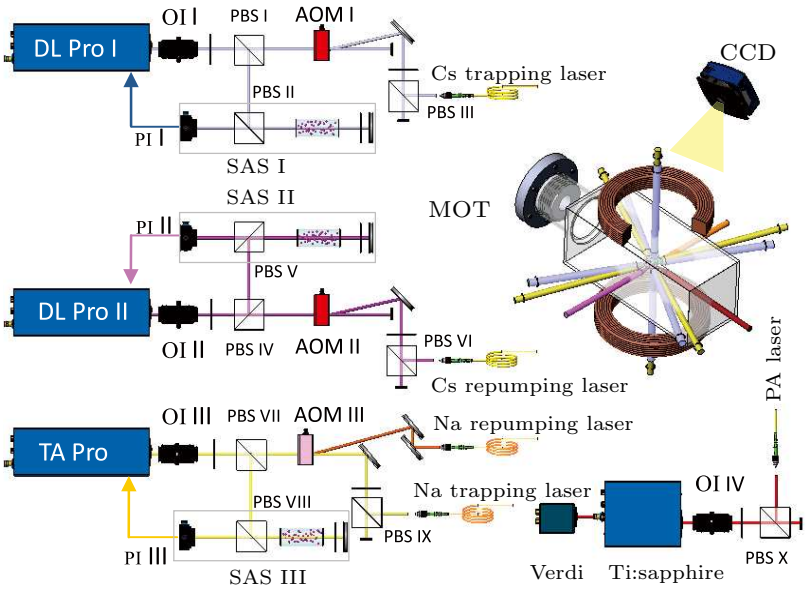


Fig. 1. (color online) Experimental setup. The Na and Cs ultracold atom samples are trapped in a dual-species MOT. SAS: saturation absorption spectrum; AOM: acousto–optic modulator; PBS: polarization beam splitter; PI: probe instrument; CCD: charge-coupled device; and OI: optical isolator.

In our experiments, the fluorescence from the trapped Cs (Na) atoms were collected by a convex lens and then detected by an avalanche photo diode (a photomultiplier) with an 852 nm (589 nm) bandpass filter. The direct fluorescence detection was usually not satisfying because noise arisen from the stray fluorescence submerged the useful signal. Our experiments[23] used the lock-in method, which is based on modulating the fluorescence of the ultracold atom, to improve the detection sensitivity of the trap-loss spectroscopy. A modulation frequency of 3.4 kHz (3.2 kHz) was used for the fluorescence from the trapped Cs (Na) atoms, and this frequency was also used to stabilize the trapping laser frequency. The modulated fluorescence was demodulated with a lock-in amplifier (Stanford Research SR830) and recorded by a computer. The uncertainty was mainly from the frequency drifts of the trapping laser, the power broadening, and the indistinguishable hyperfine structures. All these factors contributed to a maximum uncertainty of 0.003 cm^{-1}.

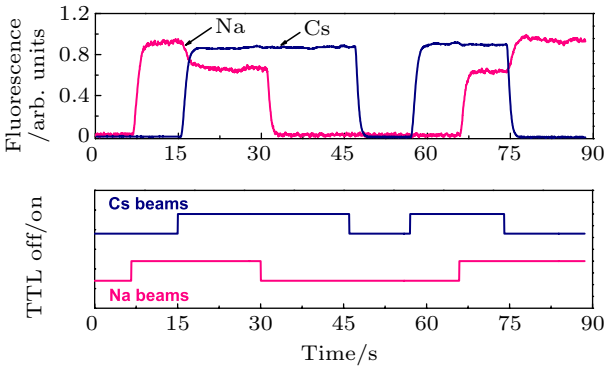


Fig. 2. (color online) Typical loading sequence for the dual-species ^{23}Na–^{133}Cs MOT. Trapping of Na (pink curve) and Cs (blue curve) is controlled by switching the corresponding trapping and repumping beams off or on.

Figure 2 demonstrates the typical fluorescence signals from the dual-species Na–Cs MOT according to the following loading sequence. The trapping lights for Cs and Na were blocked and none of the MOTs were loaded at the beginning. At $t = 6$ s, the Na beams were unblocked, which allowed the Na MOT to load. After the Na MOT reached a steady state, the Cs beams were unblocked at $t = 15$ s, which then allowed the Cs MOT to load along with the Na MOT. The number of Na atoms was gradually reduced in the presence of the Cs MOT until a new steady state was reached. At $t = 30$ s, the Na MOT was removed by extinguishing the Na beams; however, the number of Cs atoms was not affected. The Cs beams were blocked to remove the Cs MOT at $t = 46$ s. The loading sequence was then reversed.

The formation of NaCs molecules was realized in the PA process, whose resonance led to losses for both the Na and Cs atoms from the MOT, and thus, the MOT fluorescence decreased. However, the PA-induced loss in the atomic fluorescence for Cs, which was monitored simultaneously with the atomic fluorescence for Na, was hardly distinguishable during the photoassociation process. The main reason could be that the loss of Cs atoms, caused by the formation of the heteronuclear $^{23}Na^{133}Cs$ molecules, was not sufficient to affect the total Cs atomic fluorescence. Therefore, the trap-loss spectroscopy of ultracold polar $^{23}Na^{133}Cs$ molecules was detected and demonstrated by monitoring the Na atomic signals.

3. Results and discussion

In this paper, the PA spectra below the $(3S_{1/2} + 6P_{3/2})$ asymptote, i.e., red detuned from the cesium D_2 line at 852 nm, are obtained. The trap-loss technology is employed to obtain the PA spectra of the excited state of the NaCs molecules. Figure 3 demonstrates two typical trap-loss spectra for the vibrational levels in the molecular long-range $c^3\Sigma^+$ state $\upsilon = 61$, 66 for ultracold polar NaCs with rotational quantum numbers $J = 1$–3. The high-resolution PA spectra, with the rich rotational structures, provide the possibility to study the molecular constants. For a heteronuclear bi-alkali molecule, the coefficient C_3 is zero in the long-range regime, thus the long-range potential energy curve behaves asymptotically as $V(R) = -C_6/R_6 - C_8/R_8 - \cdots$, where R is the internuclear separation. The potential curve is then dominated by $-C_6/R_6$ for large interatomic distances when ignoring C_8 and higher order terms. The long-range molecular coefficient C_6, which depends on the radial dipole moment matrix element between the atomic s and p states, can be extracted from the obtained spectra.[24]

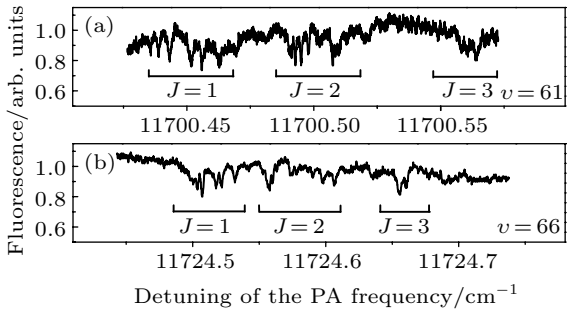


Fig. 3. Two typical PA spectra of the $c^3\Sigma^+$ state, where (a) $\upsilon = 61$, (b) $\upsilon = 66$ with rotational quantum numbers $J = 1$–3.

To extract C_6, we use the semi-classical LeRoy–Bernstein (LRB) formula[21]

$$D - E_\upsilon = A_6(\upsilon - \upsilon_D)^3, \tag{1}$$

where

$$A_6 = \frac{16\sqrt{2}}{B(2/3, 1/2)^3 \mu^{3/2} C_6^{1/2}} \pi^3 \hbar^3, \tag{2}$$

D is the dissociation energy, E_υ is the energy of the υ-th vibrational level in the $J = 0$ rotational state, υ is the vibrational quantum number from the dissociation limit, υ_D ($0 < \upsilon_D < 1$) is the vibrational quantum number at dissociation, $-(D - E_\upsilon)$

is the binding energy, μ is the reduced mass of NaCs, and B is the Beta function ($B(2/3,1/2)=2.5871$).

Figure 4 shows five typical trap-loss spectra for the molecular long-range $c^3\Sigma^+$ state of the ultracold polar NaCs when the rotational quantum number is $J=1$ and the vibrational levels are $\upsilon=61$, 62, 64, 65, and 66. They are red detuned from the $(3S_{1/2}+6P_{3/2})$ dissociation limit by ~ 31.732 cm^{-1}, ~ 25.205 cm^{-1}, ~ 14.821 cm^{-1}, ~ 10.769 cm^{-1}, and ~ 7.665 cm^{-1}, respectively. The maximum loss ratio for the signal is up to 0.40. The PA laser scanning rate is set at as small as 5 MHz/s, and the intensity of the PA laser is 500 W/cm^2. For consistency, we keep all the experimental conditions unaltered during the experiments. The resonance positions are listed in Table 1, and all the measurements are referenced to Cs's atomic hyperfine resonance transition $6S_{1/2}(F=4)\rightarrow 6P_{3/2}(F'=5)$, which corresponds to a wave number of 11732.176 cm^{-1}. For comparison, the values for the corresponding vibrational states measured by Zabawa *et al.*[25] are shown in Table 1. In Ref. [25], Zabawa reported the observation of several resonances using the ionization detection technique. The experimental results from the two groups show good agreement.

Table 1. The experimental PA resonance frequencies of different vibrational levels in the $c^3\Sigma^+$ electronic state are listed with the values from Zabawa's work.[25] The corresponding binding energies for the vibrational levels are also provided.

υ	This work		Ref. [25]	
	E_υ/cm^{-1}	$D-E_\upsilon$/cm^{-1}	E_υ/cm^{-1}	$D-E_\upsilon$/cm^{-1}
61	11700.445	31.731	11700.513	31.733
62	11706.971	25.205	11707.037	25.201
64	11717.355	14.821	11717.380	14.820
65	11721.406	10.770	11721.391	10.766
66	11724.511	7.665	11724.556	7.667

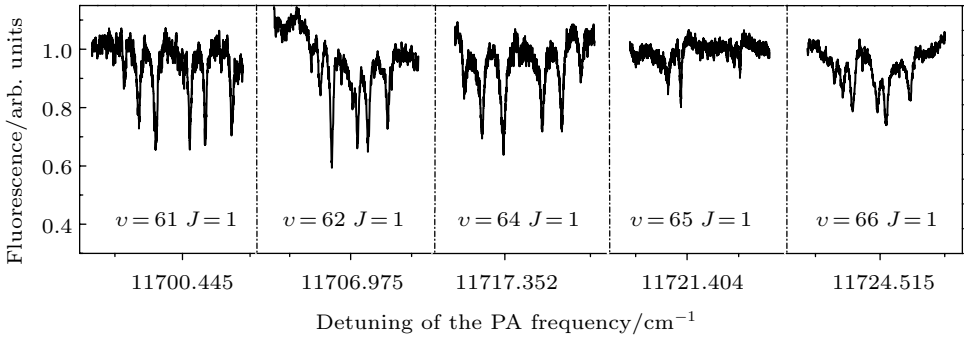


Fig. 4. Trap-loss spectra of the $c^3\Sigma^+$ electronic state with a rotational quantum number $J=1$ and different vibrational levels $\upsilon=61$, 62, 64, 65, and 66.

We fit the data in Table 1 to obtain C_6. A linear fit of the long-range parts of the $c^3\Sigma^+$ state to the LeRoy–Bernstein expression for C_6 is shown in Fig. 5, and a good linearity is illustrated. The inset is a magnification of the data near the vertical axis. The C_6 for the $c^3\Sigma^+$ state is determined to be 9261 ± 172 a.u. in our work, while a value of 9284 a.u. was obtained in Ref. [25]. The uncertainty is mainly due to a possible systematic error caused by the measurement of the wavelength meter and the errors in the determination of the resonant positions. The theoretical values of C_6 were calculated to be 18353 a.u. and 14940 a.u. by Marinescu and Sadeghpour[26] and Movre *et al.*,[27] respectively. For comparison, we list the experimental and theoretical values for NaCs's $c^3\Sigma^+$ state in Table 2. We find that the current value is in good agreement with the experimental value measured by Zabawa.[25]

Table 2. The C_6 values (in atomic units) obtained from the present work, the experiment in Ref. [25], and the theoretical calculations in Refs. [26] and [27].

Source	Year	C_6 for $c^3\Sigma^+$
This work	2017	9261 ± 172
Experiment[25]	2012	9284
Theory[26]	1999	18353
Theory[27]	1985	14940

However, the differences between the experimental and theoretical C_6 values are relatively large. The experimental values are smaller than the theoretical ones. These large discrepancies could be explained by the severe perturbations between the rovibrational levels of $\upsilon>25$ and by the neighboring $B^1\Pi$ state.[16]

The coefficient C_6 is often used to obtain the long-range molecular potential energy curve. In the LeRoy–Bernstein model, the observed successive vibrational levels are a characteristic of the long-range molecular potential energy curve, which is usually asymptotical with a $-C_6/R_6$ form. In terms of $V(R)=-C_6/R_6$, the empirical potential energy curve for the $c^3\Sigma^+$ states below the $(3S_{1/2}+6P_{3/2})$ asymptote is shown in Fig. 6. The potential curves obtained using the LeRoy–Bernstein model are defined only at the right-hand turning points of the observed vibrational levels. The curves in different colors are derived from the experimental values of this work (red dashed line) and the work in Ref. [25] (green line), and the theoretical values from Refs. [26] (blue line) and [27] (black line). The empirical potential energy curve for the molecular long-range $c^3\Sigma^+$ state in ultracold polar NaCs is de-

rived from our experimentally measured data.

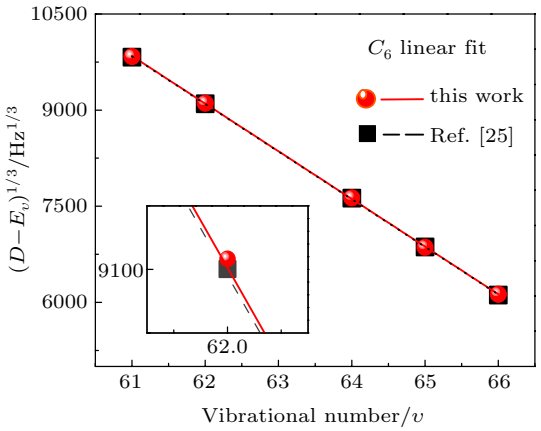


Fig. 5. (color online) The linear fit of the $c^3\Sigma^+$ levels to the LeRoy–Bernstein expression to obtain the coefficient C_6. The inset is a magnification of the date near the vertical axis.

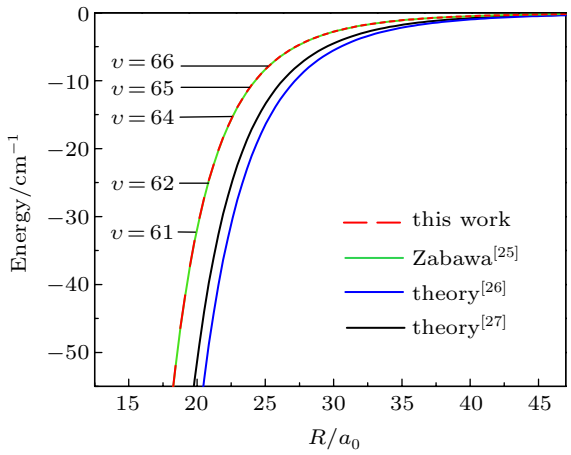


Fig. 6. (color online) The long-range parts of the potential energy curves for the $c^3\Sigma^+$ state are shown with values for C_6 obtained from our experiment (red dashed line), the experiment by Zabawa[25] (green line), and the theoretical calculations in Refs. [26] (blue line) and [27] (black line). The value of zero in the vertical coordinate represents NaCs's $(3S_{1/2}+6P_{3/2})$ asymptote (11732.176 cm^{-1}).

4. Conclusion

We have presented the PA spectra of the long-range state below the $(3S_{1/2}+6P_{3/2})$ asymptote for ultracold NaCs molecules using trap-loss detection. Five PA resonances with hyperfine structures were observed with a reasonable resolution and were identified as the $c^3\Sigma^+$ state. By fitting the experimental data to the semi-classical LeRoy–Bernstein formula, the long-range molecular coefficient C_6 was obtained as 9261 ± 172 a.u. for the $c^3\Sigma^+$ state. The experimental value shows good agreement with the result from Ref. [25], but both experimental values are smaller than the theoretical results reported in Refs. [26] and [27]. The molecular potential energy curve in the long-range region was presented based on the obtained C_6 coefficient. The trap-loss spectroscopy has proven to be a valuable method for obtaining interesting spectroscopic information. However, further studies are needed to study predissociation and second-order perturbation, which result in observations of additional levels, as well as to extract the long-range coefficients with a higher precision.

References

[1] Krems R V 2008 *Phys. Chem. Chem. Phys.* **10** 4079
[2] Roy R, Green A, Bowler R and Gupta S 2017 *Phys. Rev. Lett.* **118** 055301
[3] Flambaum V V and Kozlov M G 2007 *Phys. Rev. Lett.* **99** 150801
[4] DeMille D 2002 *Phys. Rev. Lett.* **88** 067901
[5] Aikawa K, Akamatsu D, Hayashi M, Oasa K, Kobayashi J, Naidon P, Kishimoto T, Ueda M and Inouye S 2010 *Phys. Rev. Lett.* **105** 203001
[6] Deiglmayr J, Grochola A, Repp M, Mörtlbauer K, Glück C, Lange J, Dulieu O, Wester R and Weidemüller M 2008 *Phys. Rev. Lett.* **101** 133004
[7] Chang X F, Ji Z H, Yuan J P, Zhao Y T, Yang Y G, Xiao L T and Jia S T 2013 *Chin. Phys. B* **22** 093701
[8] Wu J Z, Ma J, Ji Z H, Zhang Y C, Li Y Q, Wang L R, Zhao Y T, Xiao L T and Jia S T 2012 *Chin. Phys. B* **21** 093701
[9] Li Y Q, Ma J, Wu J Z, Zhang Y C, Zhao Y T, Wang L R, Xiao L T and Jia S T 2012 *Chin. Phys. B* **21** 043404
[10] Ma J, Li Y Q, Liu W L, Chen P, Feng G S, Hu C Y, Wu J Z, Xiao L T and Jia S T 2014 *Opt. Express* **22** 3754
[11] DeMille D, Sainis S, Sage J, Bergeman T, Kotochigova S and Tiesinga E 2008 *Phys. Rev. Lett.* **100** 043202
[12] Aymar M and Dulieu O 2005 *J. Chem. Phys.* **122** 204302
[13] Haimberger C, Kleinert J, Bhattacharya M and Bigelow N P 2004 *Phys. Rev. A* **70** 021402(R)
[14] Zabawa P, Wakim A, Haruza M and Bigelow N P 2011 *Phys. Rev. A* **84** 061401(R)
[15] Grochola A, Kowalczyk P, Szczepkowski J, Jastrzebski W, Wakim A, Zabawa P and Bigelow N P 2011 *Phys. Rev. A* **84** 012507
[16] Wakim A, Zabawa P and Bigelow N P 2011 *Phys. Chem. Chem. Phys.* **13** 18887
[17] Tiesinga E, Jones K M, Lett P D, Volz U, Williams C J and Julienne P S 2005 *Phys. Rev. A* **71** 052703
[18] Wu J Z, Ma J, Zhang Y C, Li Y Q, Wang L R, Zhao Y T, Chen G, Xiao L T and Jia S T 2011 *Phys. Chem. Chem. Phys.* **13** 18921
[19] Liu W L, Wu J Z, Ma J, Li P, Sovkov V B, Xiao L T and Jia S T 2016 *Phys. Rev. A* **94** 032518
[20] Liu W L, Wang X F, Wu J Z, Su X L, Wang S, Sovkov V B, Ma J, Xiao L T and Jia S T 2017 *Phys. Rev. A* **96** 022504
[21] LeRoy R J and Bernstein R B 1970 *J. Chem. Phys.* **52** 3869
[22] Shaffer J P, Chalupczak W and Bigelow N P 1999 *Phys. Rev. A* **60** 3365
[23] Ma J, Wang L R, Zhao Y T, Xiao L T and Jia S T 2009 *J. Mol. Spectrosc.* **255** 106
[24] Abraham E R I, Ritchie N W M, McAlexander W I and Hulet R G 1995 *J. Chem. Phys.* **103** 7773
[25] Zabawa P J 2012 "Production of Ultracold, Absolute Vibrational Ground State NaCs Molecules", Ph. D. Dissertation (New York: University of Rochester of New York)
[26] Marinescu M and Sadeghpour H R 1999 *Phys. Rev. A* **59** 390
[27] Movre M and Beuc R 1985 *Phys. Rev. A* **31** 2957